

To appear in *Astrophys. J.*

Tentative Identification of Interstellar Dust in Nose of the Heliosphere

Priscilla C. Frisch

Department of Astronomy and Astrophysics, University of Chicago, Chicago, IL 60637.

frisch@oddjob.uchicago.edu

ABSTRACT

Observations of the weak polarization of light from nearby stars, reported by Tinbergen (1982), are consistent with polarization by small, radius $< 0.14 \mu\text{m}$, interstellar dust grains entrained in the magnetic wall of the heliosphere. The region of maximum polarization is towards ecliptic coordinates $(\lambda, \beta) \sim (295^\circ, 0^\circ)$, corresponding to $(l, b) = (20^\circ, -21^\circ)$, while the dust cone direction shows a marginally significant minimum in polarization. The direction of maximum polarization is offset along the ecliptic longitude by $\sim 35^\circ$ from the nose of the heliosphere, and extends to low ecliptic latitudes. An offset is also seen between the region with the best aligned dust grains, $\lambda \sim 281^\circ \rightarrow 330^\circ$, and the upwind direction of the undeflected large grains, $\lambda \sim 259^\circ$, $\beta \sim +8^\circ$, which are observed by Ulysses and Galileo to be flowing into the heliosphere. In the aligned-grain region, the strength of polarization anti-correlates with ecliptic latitude, indicating that the magnetic wall is predominantly at negative ecliptic latitudes. An extension of the magnetic wall to $\beta < 0^\circ$ is consistent with predictions by Linde (1998). A consistent interpretation follows if the maximum-polarization region traces the heliosphere magnetic wall in a direction inclined to the local interstellar magnetic field, B_{IS} , while the region of best-aligned dust samples the region where B_{IS} stretches smoothly over the heliosphere with maximum compression. These data are consistent with a tilt of $\sim 60^\circ$ of B_{IS} with respect to the ecliptic plane, and parallel to the galactic plane. Interstellar dust grains captured in the heliosheath may also introduce a weak, but important, large scale contaminant for the cosmic microwave background signal with a symmetry consistent with the relative tilts of B_{IS} and the ecliptic.

Subject headings: heliosphere — interstellar : dust, interstellar — dust: polarization

1. Introduction

Tinbergen’s detection of weak ($\geq 2\sigma$) polarization of light for ~ 15 nearby stars, caused by magnetically aligned interstellar dust grains in the galactic center hemisphere, has long been intriguing (Tinbergen 1982, T82). Instrumental noise may introduce random weak polarization, and the significance of these polarization data results partially from the consistent polarization position angles for objects in a small region near the ecliptic plane (see Fig. 6 of T82 and Fig. 2 of Frisch 2003). T82 found the position angles to be consistent with a galactic magnetic field directed toward $l \sim 70^\circ$, which is consistent with the $l \sim 80^\circ$ local field direction found from polarization measurements of more distant stars (Heiles 1976). The location of these magnetically aligned interstellar dust grains (ISDGs) coincides with the nearest interstellar material (ISM) in the galactic center hemisphere (e.g. Bruhweiler & Kondo 1982; Frisch & York 1983).

Previous discussions of the T82 data found little increase in polarization with star distance, indicating the grains are close to the Sun (Frisch 1990; Frisch & Slavin 2005). The regions of strongest polarization and most uniform position angle are concentrated in the ecliptic plane near the heliosphere nose region (Frisch 2003). Ulysses, Galileo, and Cassini observe interstellar dust grains flowing into the heliosphere from the heliosphere nose. The grains capable of polarizing starlight, radius $a > 0.05 \mu\text{m}$, are part of the population of grains with $a < 0.1 - 0.2 \mu\text{m}$ that are filtered at the heliopause (Baguhl et al. 1996; Linde 1998; Landgraf 2000; Frisch et al. 1999, L00,F99).

In this note I argue that the T82 polarization data are consistent with polarization by charged interstellar dust grains trapped in, and diverted by, the interstellar magnetic field stretched over the heliosphere. Conventional grain alignment theories will need evaluation for the unique outer heliosheath magneto-hydrodynamic (MHD) configuration, where interstellar fields may be compressed by factors of four or more, and field aligned currents are present (e.g., Lazarian 2000; Linde 1998; Ratkiewicz et al. 1998; Pogorelov et al. 2004). The T82 data, together with the 3 kHz signals detected by Voyager in the outer heliosphere (Kurth & Gurnett 2003; Cairns 2004), represent the primary evidence for the interstellar magnetic field direction at the solar location and are both consistent with a field direction towards $l \sim 80^\circ$.¹ If my interpretation is correct, sensitive polarization observations over the 22-year magnetic solar cycle should monitor the outer heliosheath and detect variations in the interactions of these charged grains with the heliosphere.

¹After this paper was submitted, a discussion of the interstellar magnetic field direction based on Ly α interplanetary glow data was presented by Lallement et al. (2005).

Small charged grains capable of polarizing starlight are magnetically coupled to the interstellar magnetic field that is excluded from the heliosphere. For reasonable estimates of the far ultraviolet radiation field, which causes photoelectric charging of the ISDGs, and interstellar magnetic field strengths greater than $1.5 \mu\text{G}$, dust grains with radii $<0.1\text{--}0.2 \mu\text{m}$ couple to the interstellar magnetic field at the heliosphere. ISDGs with radii $a > 0.05 \mu\text{m}$ provide most polarization in the diffuse ISM (Mathis 2000). Linde (1998) estimates that ISDGs with radii $a < 0.14 \mu\text{m}$ will not enter the heliosphere because of deflection through large angles in a magnetic wall, which is formed by compressed interstellar fields lines stretched over the heliosphere nose. For the case where $B_{\text{IS}} \sim 1.5 \mu\text{G}$, and a field angle of 60° with respect to the ecliptic plane, field strength increases by factors of $\sim 4\text{--}5$, or more, in the resulting magnetic wall. However, an even stronger B_{IS} is expected if magnetic and thermal energies are approximately equal in the ISM surrounding the heliosphere. For thermal energy density $E_{\text{th}}/k = 1.5nT \sim 3700 \text{ cm}^{-3} \text{ K}$, magnetic energy density $E_{\text{B}} = B_{\text{IS}}^2/8k\pi \text{ cm}^{-3} \text{ K}$, and $E_{\text{th}} \sim E_{\text{B}}$, then $B_{\text{IS}} \sim 3.6 \mu\text{G}$ for the local ISM, which has temperature and densities $T=6340 \text{ K}$, $n(\text{H}^0) \sim 0.20 \text{ cm}^{-3}$, $n(\text{H}^+) \sim 0.09 \text{ cm}^{-3}$, and $n(\text{e}^-) \sim 0.1 \text{ cm}^{-3}$ (Slavin & Frisch 2002; Frisch & Slavin 2003).

Larger ISDGs flow into the heliosphere at $\sim 26.3 \text{ km s}^{-1}$ ($\sim 5 \text{ AU/year}$) from the upwind direction, $\lambda=259^\circ$, $\beta=+8^\circ$, and have been measured at all ecliptic latitudes in the inner 5 AU of the heliosphere (e.g., Baguhl et al. 1996; Landgraf 2000; Czechowski & Mann 2003). ISDG trajectories depend on the charge-to-mass ratio and polarity of the solar magnetic cycle. Intermediate-sized charged grains, $a \sim 0.2 \mu\text{m}$, couple to the solar wind by the Lorentz force, and are alternately focused and defocused by the changing polarity of the solar-cycle. For the positively charged ISDGs, these periods coincided with grain defocusing cycles (L00). Large grains ($a > 0.5 \mu\text{m}$) are gravitationally focused downwind of the Sun leaving a trail (or “focusing cone”) of interstellar dust extending for $>10 \text{ AU}$. A similar focusing cone is seen in interstellar He^0 data (Witte 2004; Möbius et al. 2004).

The magnetic polarity of the Sun was North-positive during $\sim 1971.6\text{--}1980.2$ when the T82 data are likely to have been acquired, and again when U/G and Voyager 3 kHz data were acquired in the 1990s (e.g. Frisch et al. 2005).

2. Tinbergen Polarization Data

Tinbergen observed ~ 180 stars at 1σ levels of degree of polarization of 7×10^{-5} , and concluded that there is a region of interstellar dust creating weak polarization of the light from nearby ($<40 \text{ pc}$) stars, with the dust centered around the galactic interval of $l \sim 340^\circ \pm 40^\circ$,

$b \sim 0^\circ$. This direction is consistent with the LSR² direction of upwind flow for the cluster of local interstellar clouds (CLIC), $l=331.4^\circ$, $b=-4.9^\circ$ (and velocity $V \sim -19.4 \text{ km s}^{-1}$, Frisch et al. 2002). (The corresponding position in ecliptic coordinates is $\lambda=255.6^\circ$ and $\beta=-32.6^\circ$.) The discussion here is restricted to ~ 160 stars within 40 pc of the Sun. T82 reported Stokes parameters Q and U for three channels, I, II, III, based on filters centered near 5400, 6100, and 8000 Å, respectively, along with the averages of channels I and II. The channel I, II averages for Q , U are used in this paper (as listed in columns 10 and 11, Table 5, of T82). Polarization is given by $P = (Q^2 + U^2)^{1/2}$, and position angle in celestial coordinates $\theta_C = 0.5 \arctan(U/Q)$ (also see Heiles 2000). Note the standard convention is used for defining the angle of polarization, θ_C , so that Q is positive and U is zero when the electric vector is North-South in the equatorial (celestial) coordinate system. It is shown below that these Tinbergen data show a distinct signature which is related to the ecliptic geometry, and which is consistent with a magnetic wall in the heliosphere nose.

The T82 observations of this nearby region of enhanced weak polarization were not reproduced by a survey of ~ 400 stars, with an accuracy of $\sigma \sim 2 \cdot 10^{-4}$ (Leroy 1993, L93). Eleven stars in the T82 patch were observed in both surveys, with declinations down to -30° . Although Leroy does not confirm the T82 results, his data are not inconsistent with the T82 results. The observation dates are unclear in the original T82 and L93 papers, but it appears the T82 data were acquired in the years surrounding or following the 1975 solar minimum, whereas the L93 data were acquired near the 1990–1992 solar maximum, where the outer heliosheath configuration would have been different.

The strength of the anticorrelation between polarization and ecliptic latitude is shown in Fig. 1. It has been determined from the covariance, $C_{P\beta}$, of polarization P and ecliptic latitude β , where:

$$C_{P\beta} = \frac{1}{(N-1) * (P_{\text{var}} * \beta_{\text{var}})^{0.5}} \sum_i^N (P_i - \bar{P}) * (\beta_i - \bar{\beta}). \quad (1)$$

Here \bar{P} and P_{var} (and $\bar{\beta}$ and β_{var}) are the mean and variance of P (and β) respectively, calculated for stars in the interval $\lambda_0 \pm 20^\circ$ centered at an arbitrary ecliptic longitude λ_0 , while N is the number of stars in that interval. N ranges from 5 to 17 for the points plotted in Fig. 1. A covariance factor of ~ -0.5 is found for stars near the upwind direction, but in addition offsets between inflowing and polarizing dust grains reveal details about the interaction of the heliosphere and interstellar magnetic field (see below). The significance of this covariance is tested by performing a similar analysis, using the same star sample, but

²Here, LSR is the Local Standard of Rest as defined by the Standard solar apex motion.

with different assumptions. In the first case, an equivalent calculation of $C_{P\beta}$ is completed using galactic instead of ecliptic coordinates, and the only features appearing simultaneously (for the same λ_0) in $C_{P\beta}$, P , and θ_C are towards the galactic center (corresponding to the heliosphere nose direction), and a group of polarized stars near $(l,b)\sim(55^\circ,+55^\circ)$. For the second test, a set of values were generated for the Stokes parameters, Q and U, with values randomly distributed between 0 and 35 (corresponding to a 5σ polarization, $P = 35 \times 10^{-5}$ deg. polarization). These random polarizations were subjected to the same analysis as the real data, and the equivalent of Fig. 1 is essentially a scatter plot for P , θ_C , and $C_{P\beta}$, with no coherent patterns that depend on λ . A third test uses the 25 stars contributing to the points in the interval $\lambda_0 = 280 - 325^\circ$, which dominate the observed anticorrelation. The polarization for 13 stars with $\beta < 0$ is $P = 16.3 \pm 6.4 \times 10^{-5}$ deg, while the average polarization for the 12 stars with $\beta > 0$ is $P = 8.0 \pm 6.1 \times 10^{-5}$ deg. Applying the Student t-test to these two samples gives an estimate, at the 98% confidence level, that the polarizations for these two samples are not drawn from a single sample with randomly distributed polarizations. Thus, the anticorrelation between polarization and β , for $\lambda = 280 - 325^\circ$, appears real. This anticorrelation indicates that the polarization signal is dominated by stars with $\beta < 0^\circ$ in this interval.

Fig. 1 summarizes the properties of the polarization data for stars within 50° of the ecliptic plane. Each plotted point represents properties averaged over a 40° longitude interval, centered at an ecliptic longitude λ_0 . The longitude, λ_0 , is stepped along the ecliptic plane at intervals of 3° in order to display variations that depend on ecliptic longitude. Fig. 1, top, shows the variation in polarization, P , as a function of λ_0 . Fig. 1, middle, shows that an interval extending from $\lambda_0=281^\circ\rightarrow330^\circ$ exhibits highly aligned grains (where $\theta_C\sim-35^\circ$, for the polarization angle in celestial coordinates), and encompasses the direction of maximum polarization observed towards $\lambda\sim295^\circ$.³ In the interval showing the strongest and most consistent polarization angle ($\lambda=281^\circ\rightarrow330^\circ$), the correlation coefficient between P and β is $C_{P\beta}\sim-0.5$ (bottom panel, Fig. 1). The strength of the P — β anticorrelation for only those stars with $\beta < 0^\circ$ gives $C_{P\beta}\sim-0.7$, a maximum smoothed value of $P \sim 20 \times 10^{-5}$ degrees, and a direction of maximum P towards $\lambda\sim294^\circ\pm4^\circ$. The anomalously high values of $C_{P\beta}\sim+0.5$, found at $\lambda\sim60^\circ$, are dominated by the two non-variable stars HD 38393 (F7 V, 9 pc) and HD 40136 (F1 V, 15 pc), located near $(l,b) \sim (223^\circ,-22^\circ)$, and with $P \sim 15 \times 10^{-5}$ degrees. The central direction of the He^o cone (Fig. 1, top) corresponds to a minimum in the polarization strength, and it extends for $\sim 15^\circ$. Since grains in the dust cone are larger than typical grains which polarize optical light (Landgraf 2000), this minimum, although marginally significant, could be explained if real. The inflowing dust grains observed by Ulysses and Galileo (U/G,

³The position of $(\lambda,\beta) = (295^\circ,0^\circ)$ corresponds to $(l,b) = (20^\circ,-21^\circ)$.

Fig. 1, top) tend to be larger than grains captured in the heliosheath (F99), and have a best-fit upwind direction within $\sim 5^\circ$ of the upwind direction, as defined by He^0 data. Fig. 1 shows clearly that the region of maximum dust inflow is offset from the region of maximum dust alignment.

In contrast, if one assumes a purely interstellar origin for the polarization, and applies standard ISM values ($P/A_V < 0.03$, $A_V/E(B-V)=3.1$, and $N(\text{H})/E(B_V)=5.8 \times 10^{21} \text{ cm}^{-2}$), then a 1σ polarization corresponds to a cloud column density of $N(\text{H}) \sim 4 \times 10^{18} \text{ cm}^{-2}$ for a magnetic field perpendicular to the sightline. This value is consistent with expected amount of nearby upwind interstellar gas; for instance, toward 36 Oph $N(\text{HI})=7.1 \times 10^{17} \text{ cm}^{-2}$ (Wood et al. 2000), and the gas in this sightline may be partially ionized (Frisch 2004). This argument, in turn, implies a purely interstellar origin for the polarization, with a possible small polarization enhancement in heliosheath currents. However, in this case it is difficult to explain the ecliptic signatures on starlight polarization as shown in Figs. 1 and 2. The gas-to-dust mass ratio is, in any case, uncertain for such small reddening values.

3. Discussion

ISDG interactions with the outer heliosheath may depend on solar cycle phase. During solar minimum phases, the heliospheric $\text{HI Ly}\alpha$ glow should show a pronounced groove from the asymmetric momentum flux of the solar wind (Bzowski 2003), compared to the more symmetric (although smaller overall) heliosphere during solar maximum. These differences in heliospheric morphology will affect the interstellar magnetic field and dust interactions with the heliosphere, and may explain the lack of confirmation of the T82 data by L93.

For magnetically aligned ISDGs in space, the plane of polarization is parallel to B_{IS} , and maximum polarization will be seen for directions perpendicular to the field lines (Heiles 1976). The polarization maximum is offset by $\sim +30^\circ \pm 5^\circ$ from the heliosphere nose, and should trace thick regions of the magnetic wall where the sightline is relatively perpendicular to the field direction. The direction of B_{IS} is $l \sim 70\text{--}80^\circ$ (from Tinbergen and Heiles 1976), which indicates that B_{IS} is tilted by $\sim 60^\circ$ with respect to the ecliptic plane. The region of maximum polarization is centered near $\lambda \sim 295^\circ$, but several strongly polarized stars are seen at low latitudes between $(\lambda, \beta) \sim (280^\circ, -10^\circ)$ and $(320^\circ\text{--}40^\circ)$. The strong polarization in this region at low ecliptic latitudes, $\beta \sim -40^\circ$, may originate in the low latitude extension of the magnetic wall resulting from the tilt of B_{IS} with respect to the ecliptic plane. Linde (1998) modeled the magnetic wall for the 1996 solar minimum, and found it stronger at southern latitudes where the azimuthal components of the interstellar and interplanetary fields are parallel, as compared to the northern hemisphere where they were antiparallel.

The best aligned grains ($\lambda=281^\circ\text{--}330^\circ$) should trace compressed B_{IS} field lines which stretch smoothly around the heliosphere (Linde 1998; Pogorelov et al. 2004; Ratkiewicz et al. 1998). Although the alignment mechanism is somewhat uncertain, polarization may be enhanced in the heliosheath nose by grain charging (e.g. by the Barnett effect) and the tight coupling between the interstellar dust grains and the compressed B_{IS} (see the discussion of grain alignment in Lazarian 2000). However, detailed models of heliosphere grain alignment and trapping are required before these results can be fully understood.

In Fig. 2, the distribution of polarization strengths are plotted in ecliptic coordinates, together with the upwind direction of the interstellar dust, H° , and He^+ flows. The positions of the 3 kHz bursts are also plotted. Both the distribution of 3 kHz bursts and the alignment of the polarization directions, shown in Fig. 2 of Frisch, 2003 and Fig. 6. of T82, indicate that B_{IS} is relatively parallel to the galactic plane. This orientation corresponds to a tilt by $\sim 60^\circ$ with respect to the ecliptic plane. The inflowing dust grains observed by Ulysses and Galileo (U/G, Fig. 1, top) tend to be larger than grains captured in the heliosheath (F99), and have a best-fit upwind direction within $\sim 5^\circ$ of the upwind direction (as defined by the antipode of the He° cone). However the 2σ uncertainties on the U/G flow direction extend to smaller λ values, corresponding to $\lambda=210^\circ\rightarrow 285^\circ$. Fig. 1 shows clearly that the region of maximum dust inflow (large grains) is offset from the region of maximum dust alignment (deflected small grains). Fig. 2 shows that the direction of maximum polarization, which should trace the magnetic wall, is inclined by a large angle to the ecliptic plane. This offset between aligned and inflowing grains also indicates that dust filtration reflects the asymmetric heliosphere configuration caused by B_{IS} , with the large-grain inflow showing the heliosphere nose, and the small grains showing the magnetic configuration of the outer heliosheath.

In principle, the relative distributions of the aligned dust, dust inflow, and He° and H° upwind directions (see Fig. 2) will be understood if we impose the requirement that the filtration factors for dust, H^+ , and other charged species vary with their gyroradius in the magnetic wall. Small dust grains are excluded (radii less than $\sim 0.05\text{--}0.1\ \mu\text{m}$) and cause maximum polarization in directions parallel to B_{IS} . Large grains (radii $\gg 0.2\ \mu\text{m}$) experience minimal filtration. About 50% of the H° is filtered in the outer heliosheath. Protons are initially deflected perpendicular to B_{IS} , but become diverted around the heliosphere along with B_{IS} in the magnetic wall. In Fig. 2, the stars with the strongest polarization form a band which makes an angle of $\sim 65^\circ$ with respect to the ecliptic plane, and similar angles are seen between the offsets of the H° and He° upwind directions. It seems a good guess that this alignment traces the magnetic wall orientation caused by the distortion of B_{IS} at the heliosphere. The IBEX data on fast H° and O° neutral atoms formed in the heliosheath (McComas et al. 2004) may map out this heliosphere asymmetry driven by the interstellar

magnetic field, through observations of H° and O° fast neutrals, which have formation rates that depend on filtration factors.

Future precise observations of very weak polarization signals, with duplicate observations and using rotatable telescopes in the northern and southern hemispheres, may provide a useful monitor of the outer heliosheath region, and of the interaction between the solar and interstellar magnetic fields. Detailed models of heliosphere grain alignment and trapping are required before these results can be fully understood.

Removing contributions from foreground emission is an important element in analyzing WMAP composite maps (Bennett et al. 2003). The possibility of a weak large scale contributions from the heliosphere indicates further modeling of this emission is warranted (Frisch & Hanson 2004; Frisch & Slavin 2004). The infrared emission from heliospheric interstellar dust appears much weaker than zodiacal emission, by factors of $\sim 10^2$ (F99). However, the observed correlation with the ecliptic of the combined quadrupole-octopole signature found by Schwarz et al. (2004) in the WMAP data, supports a possible contamination from ISDGs interacting with the heliosphere. Candidates for contamination include the small polarizing grains trapped in the magnetic wall, and discussed here; current sheets in the outer heliosheath regions; or alternatively from larger heated interstellar dust interacting with the solar wind. Any contribution to the cosmic microwave background from small grains in the outer heliosheath regions should reflect the complex asymmetry of the heliosphere interacting with B_{IS} , including the magnetic wall, rather than echoing the more simple symmetry of the ecliptic plane. If the smaller grains, radii $a < 0.2 \mu\text{m}$, are responsible, the spatial distribution may show a variation with the solar cycle, such that the heliospheric contribution to the cosmic microwave signal could be recovered from sensitive polarization observations spaced throughout the 22 year magnetic solar cycle.

4. Acknowledgements

The author would like to thank NASA (grants NAG5-11005, NAG5-13107) for supporting this work.

REFERENCES

- Baguhl, M., Gruen, E., & Landgraf, M. 1996, Space Science Reviews, 78, 165
- Bennett, C. L., Hill, R. S., Hinshaw, G., Nolta, M. R., Odegard, N., Page, L., Spergel, D. N., Weiland, J. L., Wright, E. L., Halpern, M., Jarosik, N., Kogut, A., Limon, M., Meyer,

- S. S., Tucker, G. S., & Wollack, E. 2003, *ApJS*, 148, 97
- Bruhweiler, F. C. & Kondo, Y. 1982, *ApJ*, 259, 232
- Bzowski, M. 2003, *A&A*, 408, 1155
- Cairns, I. H. 2004, in *AIP Conf. Proc. 719: Physics of the Outer Heliosphere*, 381–386
- Czechowski, A. & Mann, I. 2003, *A&A*, 410, 165
- Frisch, P. C. 1990, in *Physics of the Outer Heliosphere*, ed. S. Grzedzielski & D. E. Page, 19–22
- Frisch, P. C. 2003, *J. Geophys. Res.*, 108, 11
- Frisch, P. C. 2004, in *AIP Conf. Proc. 719: Physics of the Outer Heliosphere*, 404–411
- Frisch, P. C., Dorschner, J. M., Geiss, J., Greenberg, J. M., Grün, E., Landgraf, M., Hoppe, P., Jones, A. P., Krätschmer, W., Linde, T. J., Morfill, G. E., Reach, W., Slavin, J. D., Svestka, J., Witt, A. N., & Zank, G. P. 1999, *ApJ*, 525, 492
- Frisch, P. C., Grodnicki, L., & Welty, D. E. 2002, *ApJ*, 574, 834
- Frisch, P. C. & Hanson, A. J. 2004, unpublished
- Frisch, P. C., Müller, H. R., Zank, G. P., & Lopate, C. 2005, in *Astrophysics of Life*, 21–34
- Frisch, P. C. & Slavin, J. D. 2003, *ApJ*, 594, 844
- Frisch, P. C. & Slavin, J. D. 2004, *Space Sci. Rev.*, 0000
- Frisch, P. C. & Slavin, J. D. 2005, *Adv.Sp. Res.*, in press
- Frisch, P. C. & York, D. G. 1983, *ApJ*, 271, L59
- Heiles, C. 1976, *ARA&A*, 14, 1
- . 2000, *AJ*, 119, 923
- Kurth, W. S. & Gurnett, D. A. 2003, *J. Geophys. Res.*, 108, 2
- Lallement, R., Quémerais, E., Bertaux, J. L., Ferron, S., Koutroumpa, D., & Pellinen, R. 2005, *Science*, 307, 1447
- Landgraf, M. 2000, *J. Geophys. Res.*, 105, 10303

- Lazarian, A. 2000, in ASP Conf. Ser. 215, 69
- Leroy, J. L. 1993, A&A, 274, 203
- Linde, T. J. 1998, PhD thesis, Univ. of Michigan, Ann Arbor, small
<http://hpcc.engin.umich.edu/CFD/publications>
- Möbius, E., Bzowski, M., Chalov, S., Fahr, H.-J., Gloeckler, G., Izmodenov, V., Kallenbach, R., Lallement, R., McMullin, D., Noda, H., Oka, M., Pauluhn, A., Raymond, J., Ruciński, D., Skoug, R., Terasawa, T., Thompson, W., Vallerger, J., von Steiger, R., & Witte, M. 2004, A&A, 426, 897
- Mathis, J. S. 2000, J. Geophys. Res., 10269
- McComas, D., Allegrini, F., Bochsler, P., Bzowski, M., Ćollier, M., Fahr, H., Fichtner, H., Frisch, P., Ĝunsten, H., Fuselier, S., Gloeckler, G., Gruntman, M., Ĭzmodenov, V., Knappenberger, P., Lee, M., Livi, S., Ĝitchell, D., Möbius, E., Moore, T., Reisenfeld, D., Ĥoelof, E., Schwadron, N., Wieser, M., Witte, M., Ĥurz, P., & Zank, G. 2004, in AIP Conf. Proc. 719: Physics of the Outer Heliosphere, 162–181
- Pogorelov, N. V., Zank, G. P., & Ogino, T. 2004, ApJ, 614, 1007
- Ratkiewicz, R., Barnes, A., Molvik, G. A., Spreiter, J. R., Stahara, S. S., Vinokur, M., & Venkateswaran, S. 1998, A&A, 335, 363
- Schwarz, D. J., Starkman, G. D., Huterer, D., & Copi, C. J. 2004, Phys. Rev. Let., 93, 221301
- Slavin, J. D. & Frisch, P. C. 2002, ApJ, 565, 364
- Tinbergen, J. 1982, A&A, 105, 53
- Witte, M. 2004, A&A, 426, 835
- Wood, B. E., Linsky, J. L., & Zank, G. P. 2000, ApJ, 537, 304

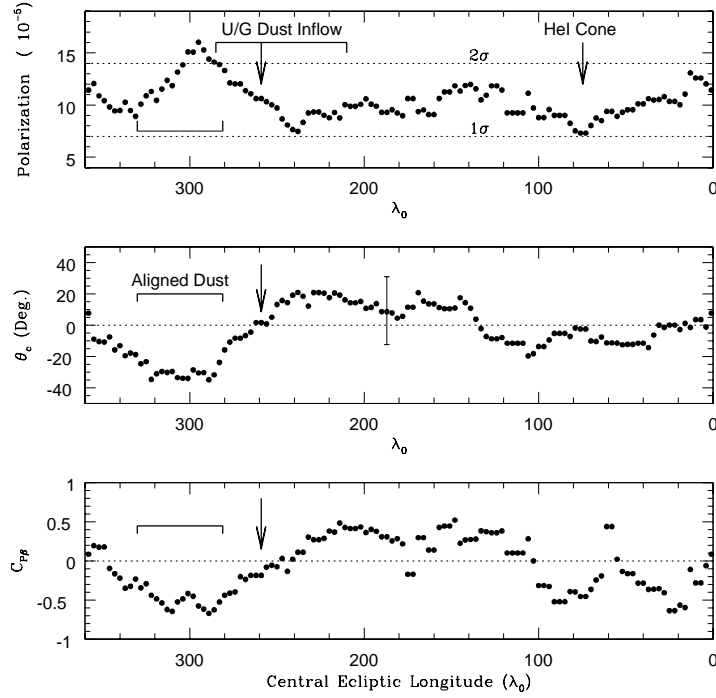


Fig. 1.— Various properties are displayed for the polarization data towards stars within 50° of the ecliptic plane. The polarization properties of stars within $\pm 20^\circ$ of a given ecliptic longitude λ_o are averaged together. The displayed points represent 3° increments in λ_o , as the direction sweeps from $\lambda=0^\circ$ (right) to $\lambda=360^\circ$ (left). Various properties of the dust polarization are clearly related to position in the ecliptic plane, such as region of maximum polarization and the angle of polarization. Top panel: The degree of polarization is shown, together with 1σ and 2σ uncertainties in the degree of polarization as quoted by Tinbergen. The λ direction and 2σ uncertainties of the best fitting inflow direction as determined from the Ulysses and Galileo observations of interstellar dust inside of the solar system are shown as an arrow and bar (respectively, from Fig. 9 in F99). The upwind gas and dust directions differ by $\sim 5^\circ$. The central direction of the He^o cone (in the downwind direction) is plotted (from Witte 2004). Middle: The polarization angle, θ_C (given in the original celestial coordinates of T82), is shown for the same set of stars. The region of $\lambda=281^\circ \rightarrow 330^\circ$ shows a consistent angle of polarization, where the dust grains have their maximum alignment. The error bar shows 1σ uncertainties on θ_C . Bottom: The correlation coefficient between degree of polarization (top panel) and ecliptic latitude is plotted as a function of the ecliptic longitude.

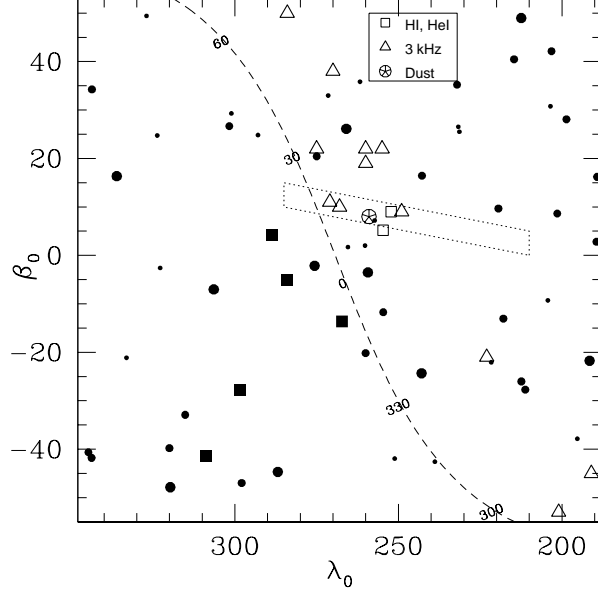


Fig. 2.— Polarization strengths are plotted in ecliptic coordinates, for stars within 40 pc and near the heliosphere nose direction. The filled circles represent polarizations of $P < 3\sigma$, and squares show $P > 3\sigma$. Small, medium and large circles are for $P < 1\sigma$, $1\sigma - 2\sigma$ and $2\sigma - 3\sigma$. Also plotted are the locations of 3 kHz emission bursts signals detected by Voyager (Kurth & Gurnett 2003), the He° and H° upwind directions (Witte 2004; Lallement et al. 2005), the inflow direction of interstellar dust as measured by Ulysses and Galileo (circled star) and an approximation of the U/G 2σ error box (dotted lines, Frisch et al. 1999). The galactic plane is shown as a dashed line. The region of maximum polarization (squares) appears to indicate the magnetic wall caused by maximum compression of interstellar B_{IS} stretched over the heliosphere. The polarization angle (not plotted) of these magnetically aligned ISDGs indicates that B_{IS} is approximately parallel to galactic plane and inclined to the ecliptic by $\sim 60^{\circ}$, while the direction of maximum polarization traces the magnetic wall.